CHROM. 15,161

EVALUATION AND COMPARISON OF REACTION DETECTORS

R. S. DEELDER*, A. T. J. M. KUIJPERS and J. H. M. VAN DEN BERG
DSM Research, Analytical Department, P.O. Box 18, 6160 MD Geleen (The Netherlands)

SUMMARY

Post-column reaction detectors are becoming increasingly popular as specific, dedicated detection systems in column liquid chromatographs. Three types of reactor are currently used: open-tubular reactors, packed-bed reactors and segmented-flow systems. The performance of these reactors was studied theoretically and investigated experimentally. A comparison was made of the performance of the various reactor types for a standard reaction. It is demonstrated that for short reaction times (*ca.* 1 min) the dispersion in each type of reactor can be reduced by an optimum design to a level that is compatible with the requirements set by modern liquid chromatographics. It is demonstrated that packed-bed reactors are preferable to open-tubular reactors with regard to dispersion and pressure drop.

For gas segmented-flow reactors, optimum performance can be obtained only when conventional debubblers are omitted.

INTRODUCTION

In liquid chromatography, post-column flow-through reactors are used as a means for improving the sensitivity and/or the selectivity of detection systems. Lower detection limits are obtained by transforming the sample components to products for which the detector has a high sensitivity. The selectivity of the detection is improved if reagents are used that are specific for a group of compounds in the sample.

Criteria for the choice of reactions that can suitably carried out in post-column reactors were discussed by Huber *et al.*[1]. As discussed elsewhere[2,3], a major problem with reaction detectors is the additional peak broadening caused by the reactor, which has an adverse effect on the performance of the system, particularly when modern efficient separation columns are used. In a properly designed post-column reactor the additional band broadening should be as low as possible to reduce the inevitable loss in resolution. Three types of reactor are currently used: open-tubular reactors, packed-bed reactors and segmented-flow systems. Rules for optimum design of these systems have been reported[4–6]. In this study we investigated the performance of these reactor types. Optimum experimental conditions were chosen on the basis of the theoretical description of the dispersion phenomena in the reactors.

BAND BROADENING IN POST-COLUMN REACTORS

In post-column reactors the fluid that is passed through carries with it a component that is modified by a chemical reaction. To predict the performance of these flow-through devices we must know (a) the rate at which the reactant R (the component to be detected) is transformed into the product P and (b) the dispersion resulting from the combination of flow pattern and molecular diffusion in the reactor. As for the reaction, we are as usually dealing with first-order reaction kinetics. The reactant will be present in the reaction mixture at low concentrations only while there is a large excess of the reagent. The heat effects of the reaction will be neglegible.

The reaction proceeds under isothermal conditions and the density of the reaction mixture does not change during the reaction. Further, we assume that the dispersion processes can be described as an axial dispersed plug-flow model[7]. The material balances for the reactant R and the reaction product P can be written as

$$\frac{\partial C_R}{\partial t} = u \cdot \frac{\partial C_R}{\partial t} + \mathbb{D}_R \cdot \frac{\partial^2 C_R}{\partial x^2} - k C_R \tag{1}$$

and

$$\frac{\partial C_P}{\partial t} = u \cdot \frac{\partial C_P}{\partial t} + \mathbb{D}_P \cdot \frac{\partial^2 C_P}{\partial x^2} + k C_P \tag{2}$$

where C_R and C_P are the concentrations of the reactant R and the product P, respectively, at axial position x and at time t, k is the reaction velocity constant and u is the mean fluid velocity in the axial direction. In these equations the dispersion due to flow pattern and molecular diffusion is expressed by the axial dispersion coefficients $\mathbb{D}_R$ and $\mathbb{D}_p$. From these equations we can obtain the response curve $C_p(x = L, t)$, the concentration distribution in the time domain of the reaction product P at the reactor outlet resulting from a pulse injection of the reactant R at $t = 0$ at the reactor inlet.

The analytical solution of these equations is straightforward if $\mathbb{D}_P = \mathbb{D}_R$. This holds approximately for segmented-flow reactors[2]. The result of tracer experiments show that in these reactors the axial dispersion is merely determined by convective mixing and that axial dispersion coefficients do not depend on the nature of the components[4].

Applying the usual approximations[8], we find

$$C_P (x = L, t) = \frac{M_R}{\sigma_{tr} F \sqrt{2\pi}} \cdot (1 - e^{-kt}) \, e^{-\frac{(t-t)^2}{2\sigma_{tr}^2}} \tag{3}$$

with

$$\sigma_{tr}^2 = 2 \, \mathbb{D} \bar{t}^3 / L^2 \tag{4}$$

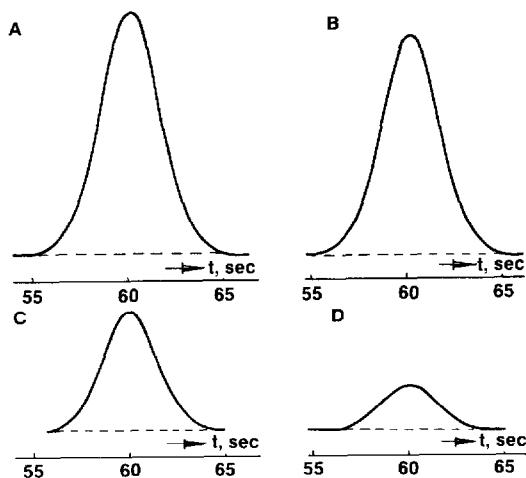$$\mathbb{D} = \mathbb{D}_P = \mathbb{D}_R$$

Fig. 1. Influence of a reaction of the peak shape in an open-tubular post-column reactor. The concentration of the reaction product at the reactor outlet was calculated from eqns. 1 and 2 for $\mathbb{D}_R = 1 \cdot 10^{-3}$ $m^2 \cdot sec^{-1}$, $\mathbb{D}_p = 2 \cdot 10^{-3} \, m^2 \cdot sec^{-1}$, $u = 0.33 \, m \cdot sec^{-1}$, $L = 18 \, m$ and $k' =$ (a) 0.1, (b) 0.03, (c) 0.01 and (d) 0.003 sec^{-1}. Peak asymmetry: (a) 1.03; (b) 1.04; (c) 1.05; (d) 1.07.

Here F is the volumetric flow-rate through the reactor, $\bar{t}$ the mean residence time ($= L/u$), L the reactor length and M_R the mass of reactant contained in the pulse-injection at $t = 0$. However, usually the axial dispersion coefficients for reactant and reaction product in open-tubular reactors or packed-bed reactors will be different, *i.e.*, $\mathbb{D}_R \neq \mathbb{D}_P$. For that case eqns. 1 and 2 were solved numerically. Fig. 1 shows some curves calculated for conditions that are typical of an open-tubular reactor. At a high degree of conversion, *i.e.*, high values for the reaction velocity constant, the peaks are nearly Gaussian. For decreasing values of k, the peak assymmetry increases, as differences in residence time correspond to increasing differences in conversion.

Both the theoretical and the experimental evaluation of the performance of a post-column reactor involve the determination of σ_{tr}^2. Let the variance, expressed in time units, of a solute band leaving the column be σ_{tc}^2, and the variance of the peak finally observed in the detector cell σ_t^2. As the variances are additive, we can write

$$\sigma_t^2 = \sigma_{tc}^2 + \sigma_{tr}^2$$

Generally, the variance σ_{tr}^2 in the reactor is calculated theoretically or measured experimentally for an inert, non-reacting component. Although the variance calculated or measured for such an inert tracer is very useful for comparing reactor performances, it cannot be used for calculating the loss in resolution between reacting components brought about in the reactor. The dispersed plug-flow model predicts symmetrical Gaussian elution curves for inert tracers at the reactor outlet when the tracer is injected as a short concentration pulse[7,8]. However, in liquid chromatography no pure Gaussian peaks are found experimentally and, as for post-column reactors, the asymmetry factor largely exceeds the values resulting from chemical reactions. First, we should think of deviations from the ideal plug flow model. As for the segmented flow reactor, the response curve for an inert tracer is known to be asym-

metric[9,10]. Moreover, symmetrical response curves may be destroyed by factors such as dead volumes in connectors, large detector volumes, imperfect injection profiles and detector time constants[11,12]. For symmetrical response curves the variance is ordinarily calculated from the peak width at a concentration corresponding to 0.607 times the concentration at the peak maximum. For asymmetric peaks, this value should be replaced by m_2, the statistical second-order central moment[11]. In practice, however, the precision of the calculation of this moment is poor[13,14], mainly as a consequence of slow drift of baselines. The precision can be improved by using an interactive procedure[14]. Yau[15] described a method for calculating the second-order central moment from the zeroth and first moments, which can usually be measured with good precision. This method holds only if the peak can be described by an exponentially modified Gaussian function[15,16].

Actually, the method allows for the calculation of both σ^2, the variance of the original Gaussian distribution, and τ, the time constant of the exponential modifier. However, caution should be exercised in characterizing post-column reactors by this procedure. The analysis of peak shapes in terms of σ and τ should rather be used to estimate peak distortion due to dead volumes, poor connections, etc., and to decide on measures for reducing this distortion. When, in spite of such measures, unreasonably high values are found for τ, the validity of the axial dispersed plug-flow model for the particular reactor seems open to question.

EXPERIMENTAL

Unless stated otherwise, tubular and packed-bed reactors were made from 316 stainless steel. Tubular reactors of 0.25 mm I.D. were used as 2.5 cm diameter coils. Packed reactors were made from 4.6 and 6 mm I.D. tubing and were filled with glass beads.

Narrow sieve fractions of these beads were purchased from Duke Scientific (Palo Alto, CA, U.S.A.), or were prepared from wide sieve range glass beads obtained from Cataphote Division/Ferro Corp. (Jackson, MS, U.S.A.) or Potters Ind. (Hasbrouck Heights, NJ, U.S.A.). No significant differences in the performance of these materials were found. For most of the experiments, mixing manifolds as described by Huber *et al.*[1] were used. For packed-bed reactors curtain-flow mixing manifolds were also used[17,18].

High-pressure pumps (Orlita DMPSK 15, Waters M 6000 or Spectra Physics SP 4000) were used as solvent and reagent delivery systems. Segmented flow reactors were made from glass tubing and were used as 5-cm coils. Segmentation air was added to the reagent stream through a capillary bubble generating system[19].

The mixing tee for adding the solvent containing the reactant to the segmented reagent stream and the debubbler were constructed such as to reduce additional dispersion.

Sampling valves (Valco CV-6-UHP, Rheodyne 7010) were used for injecting inert tracers or reactants directly into the reactor systems. As a rule, 10-μl sample loops were used. If lower injection volumes were required, the groove in the rotor of the injection valve was used as the sample loop. Some experiments in gas segmented-flow reactors were carried out without debubbling the reaction mixture ahead of the flow cell. In this instance the sample was injected into the carrier stream by means of a

syringe. At the moment of injection, the needle tip was placed as close as possible to the point at which the carrier stream was mixed with the reagent.

A variable-wavelength UV–visible detector (Zeiss PM2D) was used for most experiments. For the experiments with the gas segmented-flow reactor we used a modified fixed-wavelength detector with a low time constant[20] equipped with a 1.1 mm I.D. tubular flow cell[9] which was connected directly to the segmented-flow reactor. The detector signal was digitized by means of a digital voltmeter and the peaks were reconstructed by batchwise treatment of the data on a desk computer. The same procedure for data collection was used when calculations of second moments, deconvolution[15], etc., were required. In this study the reaction of urea (I) with p-dimethylaminobenzaldehyde, DMAB (II), was used for testing the different reactor types[21,22].
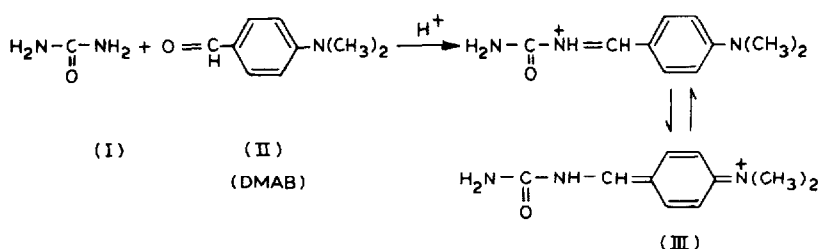
A yellow complex is formed, which can be detected at 436 nm. The reagent solution is an aqueous solution of 0.2 mol·dm^{-3} DMAB (Merck) and 0.8 mol·dm^{-3} sulphuric acid. Normally, this solution is mixed in a 1:1 ratio with water. The colour development is almost complete ($> 90\%$) for a 1-min reaction time at room temperature. The reactors were tested by injection of urea (I) and by injection of the reaction product (III). The diffusion coefficient of the reaction product in the reaction solution is $1.0 \cdot 10^{-9}$ m^2 sec^{-1} at 20°C.

DISCUSSION

Open-tubular reactors

Capillary tubes are widely used as post-column reactors. For practical reasons, these tubes are more or less tightly coiled. It is common knowledge that the coiling has a favourable influence on axial dispersion[23,24]. Low values of the additional band broadening, σ_{tr}, are obtained if narrow-bore tubes are used, although this involves high pressure drops.

For the flow conditions prevailing in open-tubular post-column reactors[5,6], the band broadening of an inert tracer is given by

$$\sigma_{tr} = \left(\frac{\kappa \, d_t^2 \, \bar{t}}{96 \, D_m}\right)^{0.5} \tag{5}$$

This equation holds only for long narrow tubes and for $\sigma_{tr} < \bar{t}$ (ref. 25). The pressure drop, Δp, can be approximated by the Poiseuille equation[5]:

$$\Delta p = \frac{512 \, \eta \, F^2 \, \bar{t}}{\pi^2 \, d_t^6} \tag{6}$$

In the equations, d_t is the internal diameter of the reactor tube, t the mean residence time of the tracer, D_m its molecular diffusion coefficient in the reactor fluid, η the viscosity of this fluid and F the volumetric flow-rate. To account for the influence of coiling on axial dispersion we further introduce the factor κ:

$$\kappa = \frac{\sigma_{tr}^2}{(\sigma_{tr}^2)_0} \leqslant 1$$

As reported earlier[6], the following empirical correlations were derived from experimental data on the dispersion of tracers in coiled tubes:

$$\kappa = 5.6 \, (Dn \cdot Sc^{0.5})^{-0.67} \text{ for } 12.5 < Dn \cdot Sc^{0.5} < 250 \tag{7}$$

$$\kappa = 1 \qquad\qquad \text{for} \qquad Dn \cdot Sc^{0.5} \leqslant 12.5 \tag{8}$$

The Dean number, Dn, is defined as $Dn = Re \, \sqrt{d_t/d_c}$, where Re is the Reynolds number and $Re = 4 \, F\varrho/\pi\eta \, d_t$, ϱ the density of the fluid and d_c the coil diameter. Sc is the dimensionless Schmidt number, defined as $Sc = \eta\varrho/D_m$. The length of the reactor, L, is calculated from

$$L = \frac{4 \, \bar{t} \, F}{\pi \, d_t^2} \tag{8}$$

An important starting point for selecting the optimum dimensions of a particular open-tubular reactor is the limit to be set to the pressure drop, Δp. Further, the flow-rate in the reactor, F, and the residence time, $\bar{t}$, are fixed by the conditions of the chromatographic separation and the reaction, respectively. Combining eqns. 5, 6 and 7, we find

$$\sigma_t \approx 0.54\varrho^{-1/6}\eta^{7/18}\lambda^{1/6} \, D_m^{-1/3}\bar{t}^{13/18}\Delta p^{-2/9} \, F^{1/9} \tag{9}$$

where $\lambda = d_t/d_c$. For any combination of ϱ, η, λ, D_m, t and F we can calculate σ_{tr} at the maximum pressure drop. Fig. 2 shows σ_{tr} as a function of t, the mean residence time of the inert tracer, for $\varrho = 1 \text{ kg} \cdot \text{dm}^{-3}$, $\eta = 1 \text{ mPa} \cdot \text{sec}$, $\lambda = 0.01$, $D_m = 10^{-9}$ $\text{m}^2 \cdot \text{sec}^{-1}$ and $F = 20 \text{ mm}^3 \cdot \text{sec}^{-1}$. These values are typical of a post-column reactor coupled to a 4.6 mm I.D. chromatographic column and with water as the solvent. The solid lines were obtained for Δp fixed at 5 and 10 MPa. Along these lines, d_t varies with $\bar{t}^{1/6}$ as shown by eqn. 6. Of course, the choice of the internal diameter of the reactor tube, d_t, is limited by the sizes of tubing commercially available. The broken line refers to 0.25 mm I.D. tubing; the line was calculated from eqns. 6 and 9. For the lower part of this curve, *i.e.*, $\bar{t} < 60$ sec, the pressure drop will be under 5 MPa, whereas pressures exceeding 10 MPa are required for $\bar{t} > 120$ sec.

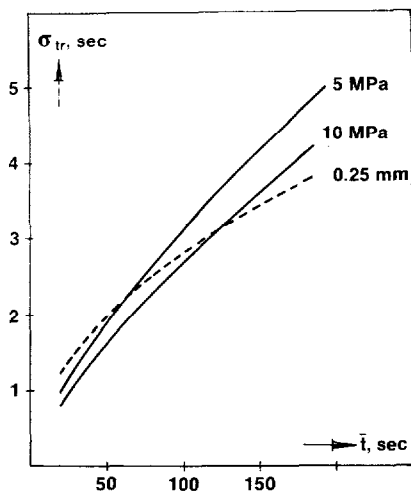The predictions from theory were verified experimentally by injecting the reac-

Fig. 2. Band broadening in coiled tubular reactors as a function of reaction time, t, at a flow-rate $F = 20$ mm$^3 \cdot$ sec^{-1}. Solid line, pressure drop fixed, tube diameter variable; broken line, tube diameter fixed, pressure drop variable.
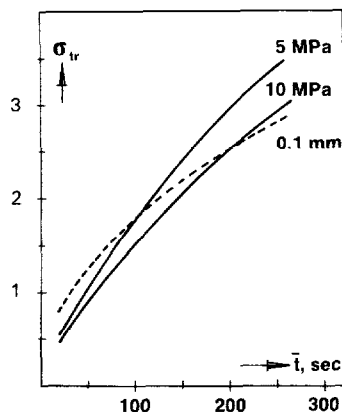
Fig. 3. Band broadening in coiled tubular reactors as a function of reaction time, t, at a flow-rate $F = 1$ mm$^3 \cdot$ sec^{-1}. Solid line, pressure drop fixed, tube diameter variable; broken line, tube diameter fixed, pressure drop variable.

tion product of urea and DMAB into a 25 m × 0.25 mm reactor, coiling ratio $d_t/d_c = 0.01$, operated at a total flow-rate of 1.2 cm$^3 \cdot$ min^{-1} which gives a residence time of 60 sec. The peaks are fairly symmetrical, the asymmetry factor[12] being about 1.15. The variance of 6.1 sec^2 also contains contributions for dispersion outside the reactor tube itself. These contributions from injector, mixing device and detector were estimated by connecting the mixing device direct to the detector. Asymmetric peaks (asymmetry factor 1.35) with a variance of about 1.2 sec^2 were obtained. The influence of the mixing tee was investigated by injection the tracer direct into the reactor tube. The contribution of the mixing device was found to be negligible. Applying a correction for dispersion originating from components outside the reactor itself we find $\sigma_{tr} \approx 2.3$ sec, which is in good agreement with the value expected theoretically (see Fig. 2).

With constant values of the residence time, $\bar{t}$, and the tube diameter, d_t, the band broadening in a coiled tubular reactor increases when the flow-rate decreases. This behaviour is a consequence of the increase of κ for lower Re values (see eqns. 5 and 7). Therefore, the tube diameter should be reduced. The calculations used for the construction of Fig. 2 were repeated for $F = 1$ mm$^3 \cdot$ sec^{-1}, a value which is typical of 1 mm I.D. columns. The results are shown in Fig. 3. Again, the solid lines refer to maximum pressures fixed at 50 and 100 atm, respectively. The broken line was obtained for 0.1 mm I.D. tubing.

An original and very simple approach for reducing axial dispersion in capillary tubes was proposed by Neue[26] and Hofmann and Halász[27]. They demonstrated that the dispersion could be reduced considerably by strong geometrical deformations of the tube. The deformations were obtained by knitting of capillaries. Obviously, only
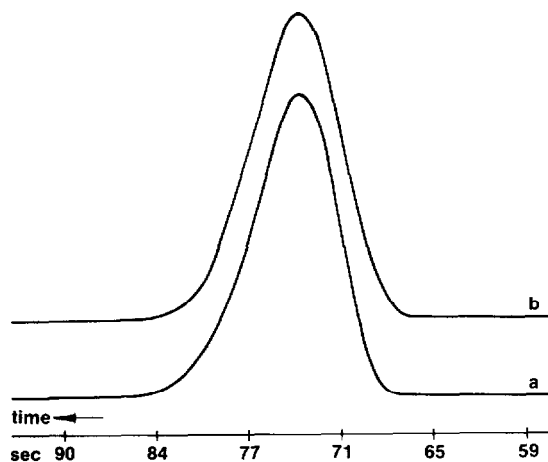
Fig. 4. Peak shape in (a) a knitted tubular reactor and (b) a tightly coiled ($\lambda = 0.05$) coiled tubular reactor. $L = 6$ m; $d_t = 0.5$ mm.

plastic tubing can be used for this type of reactor. Fig. 4 shows a peak for the urea–DMAB adduct for a 6 m × 0.5 mm PTFE reactor; the geometrical configuration was very similar to that described by Uihlein and Schwab[28]. The mean residence time was about 60 sec at a flow-rate of 20 mm$^3 \cdot$ sec^{-1}. The variance of the peak was 15.6 sec^2 or $\sigma_t = 4$ sec. The asymmetry of the peak leaves much to be desired (asymmetry factor = 1.6). For a 6 m × 0.5 mm PTFE capillary wound as a 1 cm diameter coil we found $\sigma_t \approx 4.5$ sec and a asymmetry factor of about 1.3. Band broadening in these wide-bore reactors is high compared with the 0.25 mm I.D. reactors. The knitted capillary reactor has a slight advantage over the tightly coiled tube.

Packed-bed reactors

Band broadening in columns packed with inert, non-porous particles such as glass beads is due to the influence of both axial molecular diffusion and convective mixing (eddy diffusion) in the moving fluid. We measured the plate height, H, as a function of the interstitial linear fluid velocity, u ($= L/t$), for a series of columns packed with glass beads of different average particle size, d_p. Conditions (flow-rate, column diameter, column length) were chosen so as to reduce the influence of extra-column effects on plate height. Peak asymmetry factors were 1.15 or better. Fig. 5 shows the usual plots of the reduced plate height, $h = H/d_p$, vs. the reduced velocity, $v = u \, d_p/D_m$, for different particle sizes and different column dimensions. For comparison, some data from Done and Knox[29] for unretained solutes on porous layer beads are also shown. There is good agreement among the results for the various columns and packing materials.

In chromatography, two different empirical equations are currently used for describing dispersion of unretained solutes in columns filled with inert impervious packing material. The first equation is

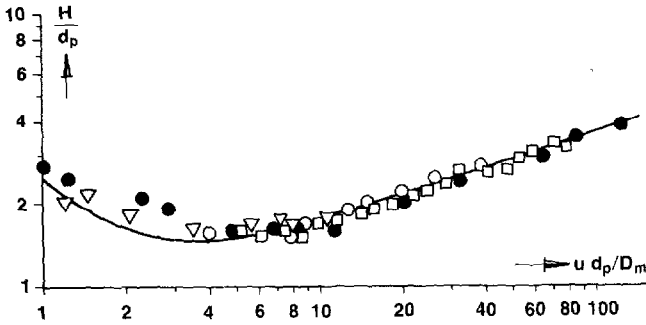$$h = 2 \, \gamma/v + \lambda_1/(1 + \lambda_2/v^{0.5}) \tag{10}$$

Fig. 5. Experimental values for h as a function of v in glass bead columns. $\bigtriangledown$, 300 mm × 6 mm, $d_p = 17$ μm; $\bigcirc$, 300 mm × 5 mm, $d_p = 45$ μm; $\square$, 480 mm × 6 mm, $d_p = 35$ μm; $\bullet$, 1 m × 2 mm, $d_p = 28$ μm[29].

where γ is the tortuosity factor and λ_1 and λ_2 are dimensionless constants depending on the geometry of the packed bed. This equation was proposed for chromatography by Huber[30]. Another, also empirical, equation proposed by Done and Knox[29] is

$$h = 2\,\gamma/v + A\,v^{0.33} \tag{11}$$

where A is a constant depending on the bed geometry.

Both equations describe equally well the experimental relationship between h and v. The full line in Fig. 5 was drawn on the basis of eqn. 10 with $\lambda_1 = 10$, $\lambda_2 = 18$ and $\gamma = 0.8$. A very similar curve is obtained from eqn. 11 for $A = 0.8$ and $\gamma = 0.8$. The latter equation is to be preferred as it contains only two empirical constants. This equation can easily be transformed into an expression suitable for calculating the additional band broadening of an inert tracer in a packed reactor:

$$\sigma_{tr} = \left(\frac{2\,\gamma\,D_m\,\bar{t}^3}{L^2} + \frac{A\,\bar{t}^{1.67}\,d_p^{1.33}}{L^{0.67}\,D_m^{0.33}} \right)^{0.5} \tag{12}$$

Low values for σ_{tr} are obtained by using long reactors packed with small particles. The pressure drop over a packed reactor, Δp, is calculated from the Darcy equation, which, in a somewhat unusual form, reads

$$\Delta p = \frac{\eta\,L^2}{k_0\,\bar{t}\,d_p^2} \tag{13}$$

where k_0 is the specific permeability of the type of packing used. A current value for k_0 for impervious spherical particles is $2 \cdot 10^{-3}$.

Fig. 6 shows a plot of σ_t vs. d_p calculated from eqn. 12 for reactor lengths of 20 and 60 cm and residence times of 1 and 2 min, respectively. A value of $1 \cdot 10^{-9}$ $m^2 \cdot sec^{-1}$ was taken for D_m. At the lower side the curves end at a point corresponding to a pressure drop of 5 MPa ($\eta = 1$ MPa · sec). It can be seen that low values of σ_{tr} can be obtained even with relatively coarse packings. Obviously, there is an advantage in using longer reactors as the same performance can be obtained for larger particles, although this does increase the pressure drop. Not only pressure drops but also
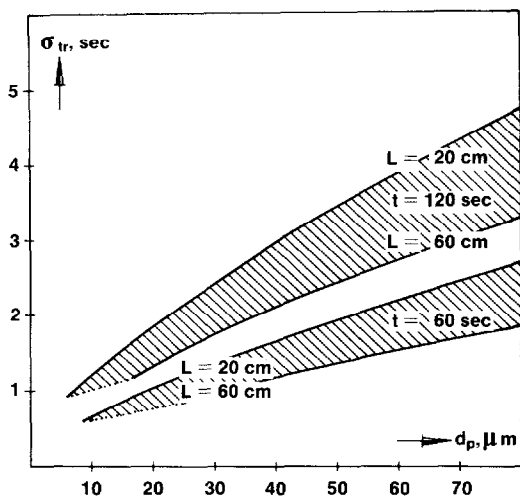
Fig. 6. Band broadening in packed bed reactors as a function of the particle diameter, d_p, for various reaction times and reactor lengths.

practical problems set a limit on the reactor length. With small particles, d_p 20 μm, slurry packing methods are applied and $L = 30$ cm seems to be the upper limit for making efficient columns. With coarser particles, dry packing methods can be used and longer columns (0.5–1 m) can be prepared without difficulty[29]. Further, the length, L, of the reactor and its internal diameter, d_r, should be chosen so as to agree with the total flow through the reactor, F:

$$L = \frac{4 \, \bar{t} \, F}{\pi \, \varepsilon \, d_r^2} \tag{14}$$

where ε is the void fraction of the reactor.

The urea–DMAB reaction product and urea were injected into a reaction detector for urea consisting of 200 $\times$ 0.46 mm I.D. 316 stainless-steel tubing packed with 40 μm glass beads; the total flow-rate was 20 mm^3 · sec^{-1} and the mean residence time was about 60 sec. Normal valve injection was used. The asymmetry of the peaks was about 1.2. When urea was injected, the resulting variance was slightly, but significantly, lower than that obtained with the urea–DMAB reactions product: 3.6 sec^2 *vs.* 4.0 sec^2. This difference may be due to the differences between the diffusion coefficients of urea and the reaction product in the reaction medium. Applying a correction for dispersion originating from components outside the reactor itself (injector, detector) we found for the urea–DMAB reaction product $\sigma_t \approx 1.7$ sec, which agrees fairly well with the value predicted from Fig. 6. For a 200 $\times$ 4.6 mm I.D. reactor packed with 17 μm glass beads the variance of the peak for the urea–DMAB reaction product was 2.5 sec^2. Applying corrections for injection and detection we found $\sigma_{tr} \approx 1.2$ sec.

Segmented-flow reactors

Segmented-flow reactors are widely used in continuous flow analysers such as

the Technicon AutoAnalyzer systems. These reactors have been used since 1969 as post-column detection systems[31]. Extensive studies[4,9] have been conducted to describe and predict dispersion phenomena in this type of reaction system but no rigorous theoretical treatment of dispersion in these reactors has been reported.

It is generally accepted that dispersion in segmented flow is brought about by slow mass transfer between the moving fluid segments and the fluid film at the tube wall. Snyder and co-workers[4,9] presented the following semi-empirical expression:

$$\sigma_{tr}^2 = \left[\frac{0.14\, d_t^{2/3}\, (F_1 + nV_g)^{5/3}\eta^{2/3}}{\sigma^{2/3}\, D_R\, F_1} + \frac{1}{n}\right] \cdot \left[\frac{2.35\, (F_1 + nV_g)^{5/3}\eta^{2/3}t}{\sigma^{2/3}\, F_1\, d_t^{4/3}}\right] \quad (14)$$

where d_t is the inner diameter of the reactor tube, F_1 the liquid flow-rate in the reactor, n the segmentation frequency, V_g the gas-bubble volume, η the viscosity, σ the surface tension of the reaction mixture and D_R an empirical radial dispersion coefficient that accounts for the slow mass transfer between the bulk of the fluid slugs and the film at the tube wall.

Values of most of the parameters in eqn. 14 (F_1, η, σ, D_R, t) are fixed by the chromatographic separation and the reaction involved. However, V_g should be chosen to be as low as possible and the combination of the tube diameter, d_t, and the segmentation frequency, n, should be selected appropriately so as to reduce $\Delta\sigma_{tr}^2$ (ref. 4).

Fig. 7 shows a plot of σ_{tr}^2 vs. length of the reactor tube, L, for the urea–DMAB complex. Values for the relevant parameters are given in Table I. As F_1, n and V_g are constant and the mean residence time, $\bar{t}$, increases linearly with L, a linear relationship between $\Delta\sigma_{tr}^2$ and L is found. The mean residence time for the 910-cm reactor is about 10 min.

Dispersion phenomena outside the reactor itself will be the cause of the intercept of Fig. 7. We pointed out earlier that additional components such as connectors, mixing tees and the debubbler may contribute significantly to the overall dispersion in
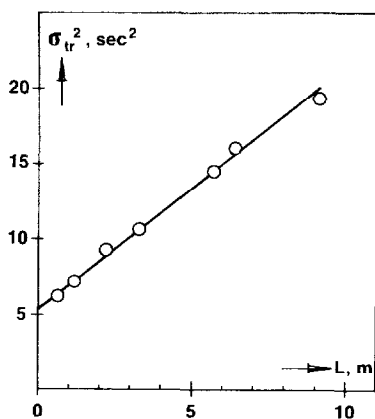

Fig. 7. Variance of the residence time distribution of a tracer in a gas segmented-flow reactor (including a debubbler) as a function of reactor length. The mean residence time in the 580-cm reactor is about 6 min. For other conditions see Table I.

TABLE I

EXPERIMENTAL CONDITIONS FOR 2 mm I.D. SEGMENTED-FLOW REACTOR

Parameter	Value
Tube diameter, d_t	2.0 mm
Liquid bubble volume, V_1	21 mm^3
Air bubble volume, V_g	18 mm^3
Segmentation frequency, n	1.2 sec^{-1}
Linear velocity	16.5 mm $\cdot$ sec^{-1}
Viscosity, η	1.1 mPa $\cdot$ sec
Surface tension, σ	72 mN $\cdot$ m^{-1}

gas segmented-flow reactors. Particularly the debubbler will have an adverse effect, as liquid holdup is required so as to prevent air segments from being sucked into the cell and some mixing between successive liquid segments can hardly be avoided. Only a minor part of the intercept, about 1.5 sec^2, can be attributed to dispersion in the injection system, the tubing to the segmented-flow reactor, the tubing from the debubbler to the detector cell and the cell itself. The greater part of the intercept, 4 sec^2, arises from mixing phenomena in the combination of the mixing tee and debubbler. This result confirms earlier findings[6,32]. On the other hand, the results are at variance with those obtained by Scholten et al.[33,34]. The different results, however, may result from the different procedures used for estimating band broadening from asymmetric peaks.

All peaks for these reactor systems show significant tailing. The peak asymmetry was found to decrease with increasing reactor length. A decrease in the peak asymmetry may be due to a decreasing influence of the mixing effects in additional components outside the reactor itself. Fig. 8 shows the peak for the 580-cm reactor. The peak can be described by an exponentially modified Gaussian function with $\sigma^\star = 2.2$ sec and $\tau^\star = 3.1$ sec, where $\sigma^\star$ is the standard deviation of the Gaussian component and $\tau^\star$ the time constant of the exponential modifier[15]. Obviously, this time constant cannot originate from components outside the reactor itself, as its value exceeds the value calculated from the intercept in Fig. 7.
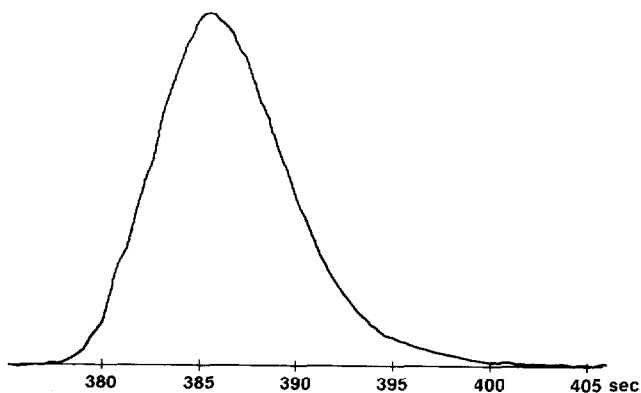

Fig. 8. Peak for urea in the 580-cm gas segmented-flow reactor. For other conditions see Table I.
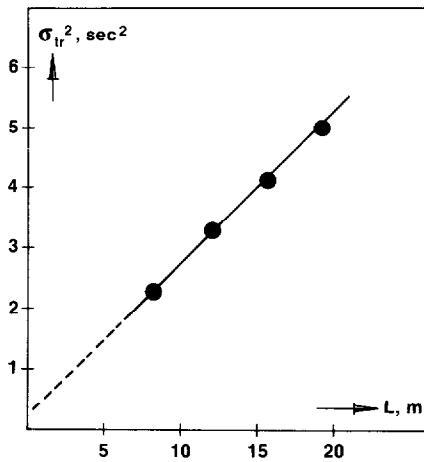
Fig. 9. Variance of the residence time distribution of a tracer in a gas segmented-flow reactor without a debubbler as a function of the reactor length. The residence time in the 19.8 m reactor is about 6 min. For other conditions see Table II.

However, theoretical studies on dispersion in segmented flow reactors point to an asymmetric residence time distribution function; the asymmetry decreases when the peak spreads over a large number of fluid segments[4,9]. This may explain the decrease of the peak asymmetry with increasing reactor length. The poor shape of the peak shown in Fig. 8 is not due to flow irregularities but results from concentration differences between the successive fluid segments. These differences are only partially levelled out by mixing in the debubbler and in the tubing between debubbler and the detector cell. The "waves" on the flanks of the peak are discernible only if the high-speed digitizing system was used for recording the detector signal. When a conventional strip-chart recorder is used the waves cannot be discerned.

Fig. 9 shows a plot of σ_{tr}^2 vs. the length of the reactor, L, for a system in which the segmented flow was red directly to the measuring cell. Values for the relevant parameters are given in Table II. A reliable construction of the peak is possible only if the volume of a liquid segment is sufficiently small compared with the peak volume. Therefore, a high segmentation frequency was chosen. The mean residence time for

TABLE II

EXPERIMENTAL CONDITIONS FOR SEGMENTED-FLOW REACTOR WITHOUT DEBUB-BLER

Parameter	Value
Tube diameter, d_t	1.13 mm
Liquid bubble volume, V_1	4.3 mm^3
Air bubble volume, V_g	4.3 mm^3
Segmentation frequency, n	5.0 sec^{-1}
Linear velocity	53.3 mm · sec^{-1}
Viscosity, η	1.1 mPa · sec
Surface tension, σ	72 mN · m^{-1}

the longest reactor ($L = 1920$ cm) was about 6 min. Once again, skewed peaks were obtained. The asymmetry, however, was less pronounced than for the 2 mm I.D. segmented-flow reactor with a debubbler and values for the asymmetry factor ranging from 1.2 to 1.4 were found. The peaks are spread over a large number of segments, which improves symmetry[4,9]. Into these reactors samples of about 0.2 mm³ were injected by means of a syringe.

For the long reactors, the peak shape obtained by this injection method was sufficiently reproducible and the relative variations of the second moment were about 15%. However, for shorter reactors these variations were found to increase and, in fact, the second moments for reactors shorter than 5 m were unreliable. Therefore, we were unable to determine experimentally with sufficient precision σ_{tr} for the standard residence time of 1 min. Under the present flow conditions (see Table II), this residence time can be obtained by using a 320-cm reactor. From Fig. 9 we can conclude that $\sigma_{tr} \approx 1$ sec for $\bar{t} = 1$ min.

The experimental results for the different reactor types are summarized in Table III. The lowest values for σ_{tr} are obtained for packed-bed reactors and segmented-flow systems. However, to come as close as possible to the theoretical performance of the latter type of reactors, the conventional debubblers should be omitted. The adverse effect of these devices has been clearly demonstrated in this study.

In order to estimate what value for σ_{tr} is acceptable in practical liquid chromatography, we consider a standard 30×0.46 cm column. The use of 5 μm packing material enables plate numbers of about 15,000 to be attained in such a column. Suppose that the column is operated at a linear velocity of 0.2 cm·sec⁻¹, which is slightly above the optimal velocity. In practice, the capacity ratio for critical separations will be at least 2, which corresponds to a retention time of 450 sec. Using these values, we find $\sigma_{tr} \approx 4$ sec. If a 10% increase in bandwith, and an equivalent loss in resolution, are considered acceptable we find $\sigma_{tr} \approx 2$ sec. For fast reactions, most of the reactors investigated meet this requirement. However, for reaction times exceeding 1–2 min the performances of all reactor types fall short of the demands of modern liquid chromatography, with the exception of gas segmented-flow reactors without a debubbler. Further development and application of these reactors will be possible only if reliable detection devices become available.

Fig. 10 shows a chromatogram of a mixture of amino acids, separated by "soap chromatography"[35]. For detection, the reaction with *o*-phthalaldehyde was

TABLE III

OBSERVED BAND BROADENING FOR STANDARD CONDITIONS

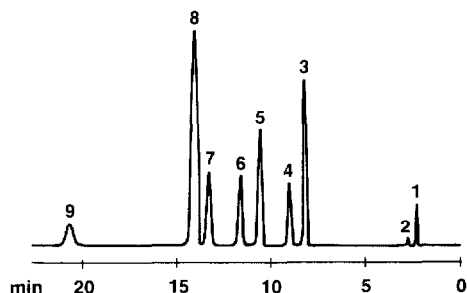| Reactor type	σ_{tr} (sec)	Δp (MPa)
Coiled tubular, 25 m × 0.25 mm	2.3	5
Coiled tubular, 6 m × 0.5 mm	4.5	0.3
Knitted tubular, 6 m × 0.5 mm	4.0	0.3
Packed bed, 20 cm × 4.6 mm, $d_p = 40$ μm	1.7	0.3
Packed bed, 20 cm × 4.6 mm, $d_p = 17$ μm	1.2	1.6
Segmented flow, 2.0 mm I.D. + debubbler★	2.2	< 0.1
Segmented flow, 1.1 mm I.D., no debubbler	1.0	< 0.1

★ $F = 25$ mm³·sec⁻¹.

Fig. 10. Chromatogram of a mixture of amino acids. Column, 15 × 0.46 cm, packed with 5 μm Li-Chrosorb RP-8. Eluent, 0.01 M phosphate buffer in water, pH 2.5, +2% n-propanol + 0.08% sodium dodecylsulphonate. Reactor, 30 × 0.46 cm, packed with 17 μm glass beads. Flow-rates: eluent, 16.7 mm^3·sec^{-1}; reagent, 16.7 mm^3·sec^{-1}. Column and reactor temperature, 25°C. Peaks: 1 = cysteic acid; 2 = taurine; 3 = methionine sulphone; 4 = aspartic acid; 5 = serine; 6 = glutamic acid; 7 = threonine; 8 = glycine; 9 = alanine.

used[36]. A 15 cm × 0.46 cm I.D. column packed with 5 μm LiChrosorb RP-8 was used.

The band broadening in the packed-bed reactor (30 cm × 0.46 cm I.D.) filled with 17 μm glass beads was measured as follows. Tyrosine, a UV-absorbing amino acid, was injected into the chromatographic column, which had been connected directly to a UV detector. The eluent had been modified by leaving out the surfactant and by adding 1-propanol in order to reduce the capacity factor for tyrosine to about 1. The variance for the tyrosine peak was measured. Then, the UV detector was replaced by a combination of the packed-bed reactor and a fluorescence detector. Tyrosine was injected again and the variance of the peak was measured. The results are given in Table IV. The increase in bandwith, σ_{tr}, due to the use of the reactor is about 1 sec.

Finally, it should be noted that the limitation of the reaction time to 1–2 min as discussed earlier does not always preclude the use of reaction detectors. Slow reactions can often be accelerated considerably by heating. When tubular or packed-bed reactors are used, the closed pressurized reactor allows the reaction mixture to be heated to temperatures that exceed the boiling point of the mixture. Fig. 11 shows a chromatogram of a mixture of sugars. Reducing carbohydrates were converted into fluorescing derivatives by reaction in slightly alkaline solution with 2-cyano-

TABLE IV

EXPERIMENTAL DETERMINATION OF THE BAND BROADENING IN THE REACTION DETECTOR FOR AMINO ACIDS

Test compound: tyrosine (capacity ratio 1.1).

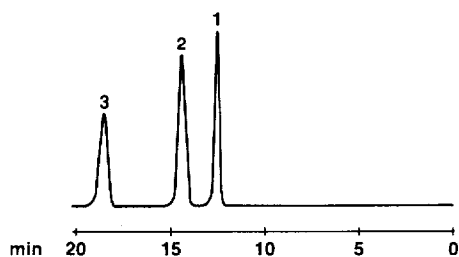| Experiment	σ_t^2 (sec^2)
(1) Column + reaction detector	3.4
(2) Column + UV detector	2.3
Increase due to reaction detector	1.1

Fig. 11. Chromatogram of a mixture of aldoses as monitored by fluorimetric post-column labelling with 2-cyanoacetamide. Column, 25 × 0.46 cm, packed with 10 μm Polygosil 100. Eluent, acetonitrile–water (80:20) + 0.01 % HPLC Amine Modifier I[38]. Reactor, 20 m × 0.25 mm, 316 stainless steel, cooler 5 m × 0.25 mm, 316 stainless steel. Reagent, 0.01 % 2-cyanoacetamide in buffer (pH 7.6) prepared from 0.2 M sodium tetraborate and 0.2 M potassium dihydrogen phosphate. Flow-rates: eluent, 12 mm$^3 \cdot$sec^{-1}; reagent, 5 mm$^3 \cdot$sec^{-1}. Column temperature, 25°C; reactor temperature, 150°C. Excitation, 331 nm; emission wavelength, 383 nm. Peaks: 1 = fructose; 2 = glucose; 3 = saccharose.

acetamide[37]. We found that this reaction can be considerably accelerated by heating the reaction mixture to 150°C. The reaction was carried out in a 20 m × 0.25 mm coiled tubular reactor ($d_c/d_t = 50$); a short capillary (5 m × 0.25 mm) was used for cooling the reaction mixture prior to entering the flow cell and for preventing the mixture from boiling. The additional band broadening, σ_{tr}, in this reaction system is about 3 sec.

REFERENCES

1 J. F. K. Huber, K. M. Jonker and H. Poppe, *Anal. Chem.*, 52 (1980) 2.
2 R. S. Deelder and P. J. H. Hendricks, *J. Chromatogr.*, 83 (1973) 343.
3 R. S. Deelder, M. G. F. Kroll and J. H. M. van den Berg, *J. Chromatogr.*, 125 (1976) 307.
4 L. R. Snyder, *J. Chromatogr.*, 125 (1976) 287.
5 R. Tijssen, *Anal. Chim. Acta*, 114 (1980) 71.
6 R. S. Deelder, M. G. F. Kroll, A. J. B. Beeren and J. H. M. van den Berg, *J. Chromatogr.*, 149 (1978) 669.
7 K. B. Bischoff and O. Levenspiel, *Chem. Eng. Sci.*, 17 (1962) 245.
8 O. Levenspiel and W. K. Smith, *Chem. Eng. Sci.*, 6 (1957) 227.
9 L. R. Snyder and H. J. Adler, *Anal. Chem.*, 48 (1976) 1017 and 1022.
10 H. Pedersen and C. Horváth, *Ind. Eng. Chem., Fundam.*, 20 (1981) 181.
11 J. C. Sternberg, *Advan. Chromatogr.*, 2 (1966) 205.
12 J. J. Kirkland, W. W. Yau, H. J. Stoklosa and C. H. Dilks, Jr., *J. Chromatogr. Sci.*, 15 (1977) 303.
13 K. H. Radeke, *Ind. Eng. Chem., Fundam.*, 20 (1981) 302.
14 M. E. van Kreveld and N. van den Hoed, *J. Chromatogr.*, 149 (1978) 71.
15 W. W. Yau, *Anal. Chem.*, 49 (1977) 395.
16 R. E. Pauls and L. B. Rodgers, *Anal. Chem.*, 49 (1977) 625.
17 C. J. Little, J. A. Whatley and A. D. Dale, *J. Chromatogr.*, 171 (1979) 63.
18 T. J. N. Webber and E. H. McKerrell, *J. Chromatogr.*, 122 (1976) 243.
19 C. Horváth, B. A. Salomon and J. M. Engasser, *Ind. Eng. Chem., Fundam.*, 12 (1973) 431.
20 R. P. W. Scott, P. Kucera and M. Munroe, *J. Chromatogr.*, 186 (1979) 475.
21 G. W. Watt and J. D. Crisp, *Anal. Chem.*, 26 (1954) 452.
22 R. C. Hoseney and K. F. Finney, *Anal. Chem.*, 36 (1964) 2154.
23 P. S. Srinivasan, S. S. Nandapurkar and T. A. Holland, *Trans. Inst. Chem. Eng. Chem. Eng.*, 46 (1968) 113.
24 C. G. Horváth, B. A. Preiss and S. R. Lipsky, *Anal. Chem.*, 39 (1967) 1422.
25 V. Ananthakrishnan, W. N. Gill and A. J. Barduhn, *AIChEJ.*, 11 (1965) 1063.

26 U. D. Neue, *Dissertation*, Saarbrücken, 1976.
27 K. Hofmann and I. Halász, *J. Chromatogr.*, 199 (1980) 3.
28 M. Uihlein and E. Schwab, *Chromatographia*, 15 (1982) 140.
29 J. N. Done and J. H. Knox, *J. Chromatogr. Sci.*, 10 (1972) 606.
30 J. F. K. Huber, *J. Chromatogr. Sci.*, 7 (1969) 85.
31 G. Ertingshausen, H. J. Adler and A. S. Reichler, *J. Chromatogr.*, 42 (1969) 355.
32 R. L. Habig, B. W. Schlein, L. Walters and R. E. Thiers, *Clin. Chem. (Winston-Salem, NC)*, 15 (1969) 1045.
33 A. H. M. T. Scholten, U. A. Th. Brinkman and R. W. Frei, *J. Chromatogr.*, 205 (1981) 229.
34 A. H. M. T. Scholten, U. A. Th. Brinkman and R. W. Frei, *J. Chromatogr.*, 218 (1981) 3.
35 J. H. Knox and G. R. Laird, *J. Chromatogr.*, 122 (1976) 17.
36 M. Roth and A. Hampaï, *J. Chromatogr.*, 83 (1973) 353.
37 S. Honda, Y. Matsuda, M. Takahashi, K. Kakehi and S. Ganno, *Anal. Chem.*, 52 (1980) 1079.
38 K. Aitzetmüller, *Chromatographia*, 13 (1980) 432.